Dongfan Li*, Hangshan Gao, Zhixun Wen, Zhenwei Li and Zhufeng Yue

The Effect of Post-heat Treatment on the Microstructures of Single Crystal DD6 Superalloy

DOI 10.1515/htmp-2015-0037
Received February 7, 2015; accepted July 28, 2015

Abstract: Various thermal cycles at the end of solution heat treatment and their influences on microstructure of single crystal superalloy DD6 were studied by experiments. During various thermal cycles, the qualitative and quantitative microstructure of samples quenched of the transformations is microscopically characterized. This completely includes the large changes in volume fraction, size distribution and morphology of gamma prime precipitate experienced in the upper temperature transformation. Noticeable deviation from the equilibrium volume fraction of γ' phase is detected in both the dissolution and precipitation processes above 1,120°C for both moderate cooling and heating rate; differences were mainly attributed to the unsteady nature of the turbulent flow. The growth and alignment of the γ' precipitates are deeply influenced by several factors, e.g. ageing time, cooling rate and quenching temperature. In addition, interesting findings such as "labyrinth" and "cluster" morphologies were observed by scanning electron microscope. During precipitation processes, the complicated microstructure evolution is illustrated by considering the consecutive equilibrium shapes of a coherent precipitate, which grows under the interaction with its neighbors and the coherency of the precipitates improves their potential to resist dissolution.

Keywords: γ/γ' phase transformation, post-heat treatment, single crystal, micro-structure, crystal growth

Introduction

The mechanical properties of single crystal superalloys are intensely influenced by the kinetics of precipitation strengthening caused by the ordering that produces the $L1_2$ crystal structure, denoted by γ', from the face-centered cubic (FCC) matrix phase-γ [1]. The morphology of the γ' precipitates has been detailedly reported and massive γ' precipitate shapes have been observed (spheres, cubes, aligned cubes, plates, short plates, doublet of short plates, octet of cubes, large plates, rafts, etc.) [2–9]. It has been figured out that most of these structures actually form under the effect of the elastic energy correlated with the lattice mismatch between the γ' precipitates and the γ matrix [10]. With regard to the wide range of morphologies reported in the literature, it appears that the shape evolution strongly depends on the alloy composition and on the heat treatment parameters [11]. From the theoretical point of view, the coherent precipitates of γ' phase in γ matrix are therefore appropriate for testing predictions of precipitate morphology and a variety of theories that explain the influence of lattice strain have been put forward to interpret the different shapes and microstructures [11–16].

Despite the numerous observations of precipitate shapes after various kind of thermal and thermal mechanical treatment, unfortunately, some of the results documented seem to be contradictory and the mechanism is not clear at present about the consecutive development of the precipitate morphology during various heat treatments. Furthermore, it is noticeable that little work has focused on the high temperature $\gamma \leftrightarrow \gamma + \gamma'$ phase transformation which contains a large γ' volume fraction and shape changes.

In order to supply with a better understanding of the microstructure evolution in the case of cooling rate and isothermal heat treatment, this work was then to experimentally research the $\gamma \leftrightarrow \gamma + \gamma'$ transformation in advanced single crystal superalloys. This paper is fundamentally related to investigation associating microstructure characterization of the phase transformation without applied stress.

Experimental details

DD6 is the second-generation single crystal superalloy developed by Beijing Institute of Aeronautical Materials

***Corresponding author: Dongfan Li,** Department of Engineering Mechanics, Northwestern Polytechnical University, Shaanxi, Xi'an 710072, PR China, E-mail: lidongfan@mail.nwpu.edu.cn
Hangshan Gao, Zhixun Wen, Zhenwei Li, Department of Engineering Mechanics, Northwestern Polytechnical University, Shaanxi, Xi'an 710072, PR China
Zhufeng Yue, Department of Engineering Mechanics, Northwestern Polytechnical University, Shaanxi, Xi'an 710072, PR China; Vehicle Structural Mechanics and Strength Technology, COSTIND Key Discipline Laboratory, Shaanxi, Xi'an 710072, PR China

and has many advantages such as high strength at elevated temperature, excellent comprehensive performance and good microstructure stability [17]. The difference in lattice parameters between the coherent γ and γ' phases is characterized by the misfit parameter $\delta = 2(a_{\gamma'} - a_{\gamma})/(a_{\gamma'} + a_{\gamma})$, where $a_{\gamma'}$ and a_{γ} are the lattice parameters of the precipitate and matrix in a non-constrained state. For the DD6 alloys, the misfit was found to be negative at high temperature. The relationship between δ values and temperature in 2% Re alloy can be approximately expressed as: $\delta = -\frac{T}{200000} - 0.0021$ for DD6 [18].

Materials

This study was carried out on the DD6, of which the chemical composition is listed in Table 1 [19]. Single crystal rods of the alloys were cast using a directional solidification method. The heat treatments of the specimens were carried out according to following heat treatment regime: (1,290°C, 1 h) + (1,300°C, 2 h) + (1,315°C, 4 h, AC) + (1,120°C, 4 h, AC) + (870°C, 32 h, AC).

It has previously been revealed that rods which do not contain any chemical segregation should be used for a more exact study of the phase transformation [20]. The homogenization condition will be referred hereafter as H4hr. The crystal orientations of the specimens were determined by Laue X-ray back reflection method, and the crystal orientation deviations of the specimens were maintained within 10° to the [001] orientation.

Heat treatments

The two types of heat treatments we used to characterize dissolution (γ + γ' → γ) are as follows: (i) continuous heating at a rate of 0.15°C/s interrupted by water cooling at different temperatures above 1,120°C; (ii) continuous heating at a rate of 0.15°C/s followed by isothermal treatments at various temperatures below the γ' transus, then water cooling. Precipitation (γ → γ + γ') was characterized by cooling samples after 30 min of isothermal treatment in the γ' field. Three different precipitation routes were used: (i) qualitatively, continuous cooling using furnace cooling (FC), air cooling (AC) and water cooling (WC); (ii) continuous cooling at a rate of 0.15°C/s interrupted at various temperatures by water cooling; (iii) continuous cooling at a rate of 0.15°C/s followed by isothermal treatments then water cooling.

Temperature control and measurements

All these treatments were carried out using a specific apparatus developed by Luoyang Sigma instrument manufacture Co., Ltd. This apparatus can easily keep specific temperature rather constant and as many as 30 periods for continuous temperature control. Meanwhile, its fine overshoot and high accuracy provide strong support for experiment. Bulk samples (3 mm × 3 mm × 2 mm) were tied to a high temperature resistance rod and put in the furnace from the hole on the back wall when the furnace reaches 1,315°C, which was used for fast heating. In order to ensure the accuracy, the samples should be as far as possible to the tip of the temperature sensor. Fast cooling was realized by removing the specimen outside the furnace at 1,315°C and then dropping into water as soon as possible. Regulating both resistance-wire heating and water cooling allows a perfect control of complex thermal cycles. The temperature was measured and controlled with a Pt-Rh thermocouple (WRP) spot welded on the surface.

Microstructure characterization

Microstructures resulting from the different heat treatments were characterized by scanning electron microscope

Table 1: Chemical composition of Ni-based single DD6 crystals/%.

C	Cr	Ni	Co	W	Mo	Al	Ta	Nb	Re	Hf
0.001~0.04	3.8~4.8	Balance	8.5~9.05	7.0~9.0	1.5~2.5	5.2~6.2	6.0~8.5	0~1.2	1.6~2.4	0.05~1.5
Other elements ≤										
Ti	**Fe**	**B**	**Zr**	**Mn**	**Si**	**P**	**Cu**	**S**	**Mg**	
0.10	0.30	0.02	0.10	0.15	0.20	0.018	0.10	0.004	0.003	

(SEM). The surfaces observed were generally perpendicular to the rod axis (i.e. parallel to a (001) plane). The surfaces for the SEM observations were mechanically polished, then etched for about 3 s in a solution of glycerol, hydrofluoric acid and nitric acid in the proportion 3:2:1. Attention should be paid that the solution needs to be put in a closed vessel since it will be expired in a week after use. Aimed at an efficient quicker view, observations were carried out on both QUANTA600F-SEM and JSM6700F-SEM microscope for two sets. Taking the uniform distribution of γ' phase into account after solution treatment, it is adequately reasonable to assume that the content of γ' precipitates is approximately the same in every layer of samples, that is, we can only just count up the area fraction of γ' precipitates on the SEM micrographs to substitute the volume fraction of the whole samples. On the basis of this assumption, area fraction of γ' precipitates at a given temperature were measured by a software (called "Image J") on SEM micrographs.

Results: effects of heat treatment on microstructure and properties

The effects of heat treatment, specifically quenching and ageing on the microstructure evolution of the nickel-based superalloy DD6 are now studied in detail, with emphasis placed on four aspects: (i) volume fraction, (ii) gamma prime size distribution, (iii) microstructure evolution during precipitation, (iv) dissolution. To this end, bulk specimens subjected to different heat treatment conditions have been analyzed using SEM microscopy to describe the size of the precipitates. Image J was used to count and measure the precipitates.

Volume fraction

Figure 1 shows quantitative image analysis results for the H4hr DD6 alloy. The volume fraction parameter of γ' phase, at different temperatures on heating at (0.15°C/s), cooling at (0.15°C/s) or after subsequent isothermal heat treatments – leading to approaching equilibrium conditions – is shown in Figure 1(a) in the temperature range between 1,170 and 1,260°C. It can be seen that the γ' volume fraction varies significantly within the first 90°C below the solvus. It is also clear that the volume fraction of γ' phase on heating and cooling is always far from the equilibrium fraction, especially for the heating condition. This is confirmed by the evolution of the volume fraction of γ' phase with time for the temperature of 1,240°C shown in Figure 1(b). The volume fraction approaches approximately 65% with the decreasing temperature. Luckily, the results (see Figure 1(a)) were in reasonable agreement with the China Aeronautical Materials Handbook [21].

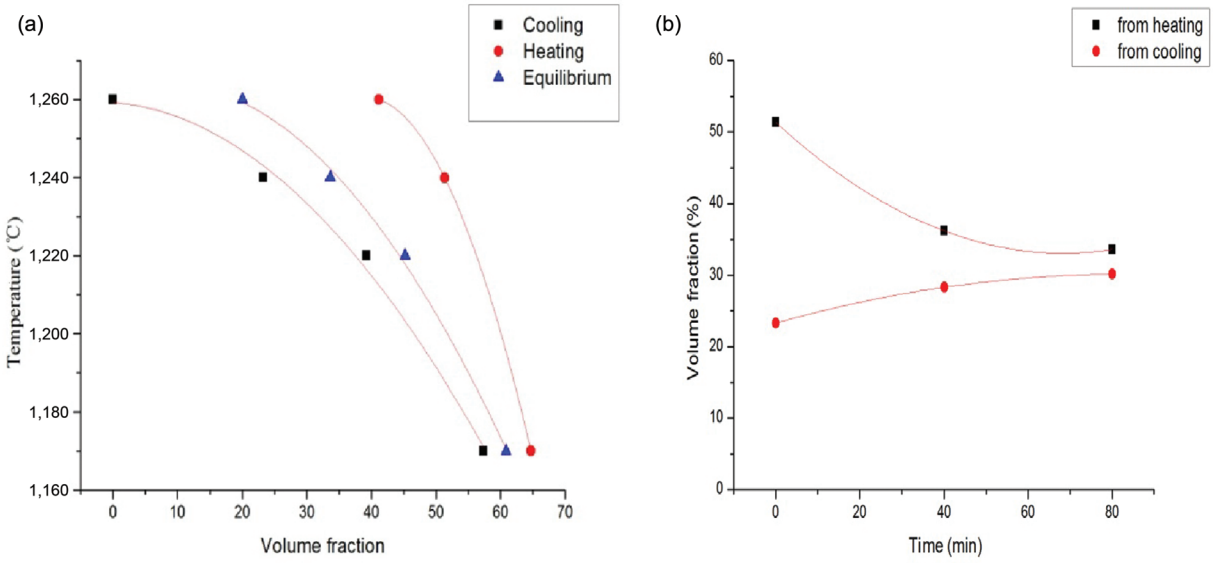

Figure 1: Quantitative image analysis for H4hr DD6: (a) Evolution of the relative volume fraction of γ' phase with temperature under cooling and heating at 0.15°C/s as well as equilibrium conditions. (b) Evolution of the volume fraction of γ' phase during ageing at 1,240°C subsequently to continuous cooling from 1,315°C (0.15°C/s) or continuous heating from room temperature (0.15°C/s).

Gamma prime size distribution

Ageing

The heat treatment consisted of a continuous heating at 0.15°C/s from room temperature to 1,260°C, followed by isothermal treatment for 40 or 80 min and then water cooling. Typical precipitate size in the as quenched structure and its evolution as a function of ageing time is presented in Figure 2 for the DD6. Here, micrograph (a) presents the "as quenched" structure that shows a rather interesting distribution of γ' with a spherical "labyrinth morphologies". Figure 2(b)–(c) shows the evolution of the structure with ageing time: the precipitate size increases slowly in the first 40 min, followed by a sharp coarsening, with mostly an increase in order and a reduction in the channel width.

Cooling rates

Figure 3 shows micrographs of the structure resulting from the γ field in the case of DD6 alloy. Their shape and size distributions are intensely dependent on the cooling conditions. Figure 4 presents the particle number and volume fraction of γ' precipitates in different cooling rates. These two figures reveal that higher cooling rates make less γ' precipitates, simultaneously, Figure 3(b) (air cooling) has the smallest average edge length of γ' precipitates, of which the largest one is observed in Figure 3(c). Namely, lower cooling rate make for the growth as well as an ordered arrangement of γ' precipitates. For water cooling (see Figure 3(a)) as well as air cooling (see Figure 3(b)), the γ' precipitates were so tiny with a chaotic arrangement. Comparatively, for furnace cooling (see Figure 3(c)), the microstructure observed by SEM was a mixture (with larger size) of cubes, groups of cubes and intermediate more complex shapes (arrowed), which will be discussed later. Compared with Figure 3(c), a large number of cross-shaped dark stripes proved to be primary dendritic were observed in both Figure 3(a) and (b), which were just like crisscross of paths in fields. Apart from ageing factor, the order of the structure also correlates with cooling rates. In fact, by comparing the samples with different cooling rates (see Figure 5), one can visually

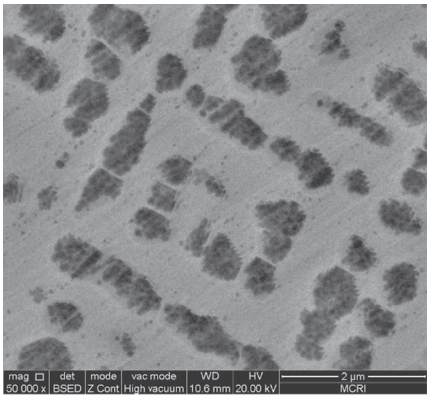

(a)

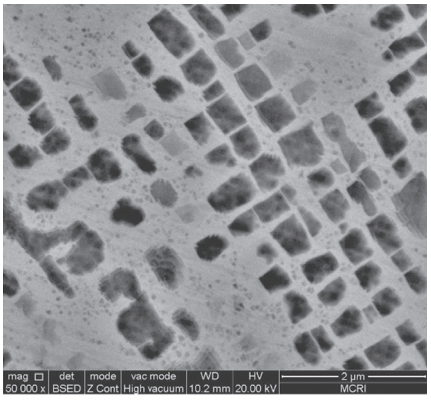

(b)

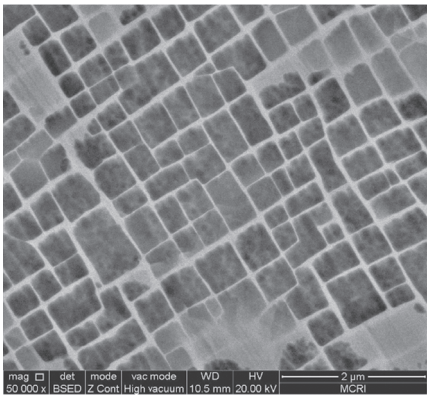

(c)

Figure 2: Evolution of precipitate microstructure with isothermal ageing at 1,260°C. (a) DD6 as water quenched; (b) After 40 min of isothermal ageing; (c) After 80 min of isothermal ageing.

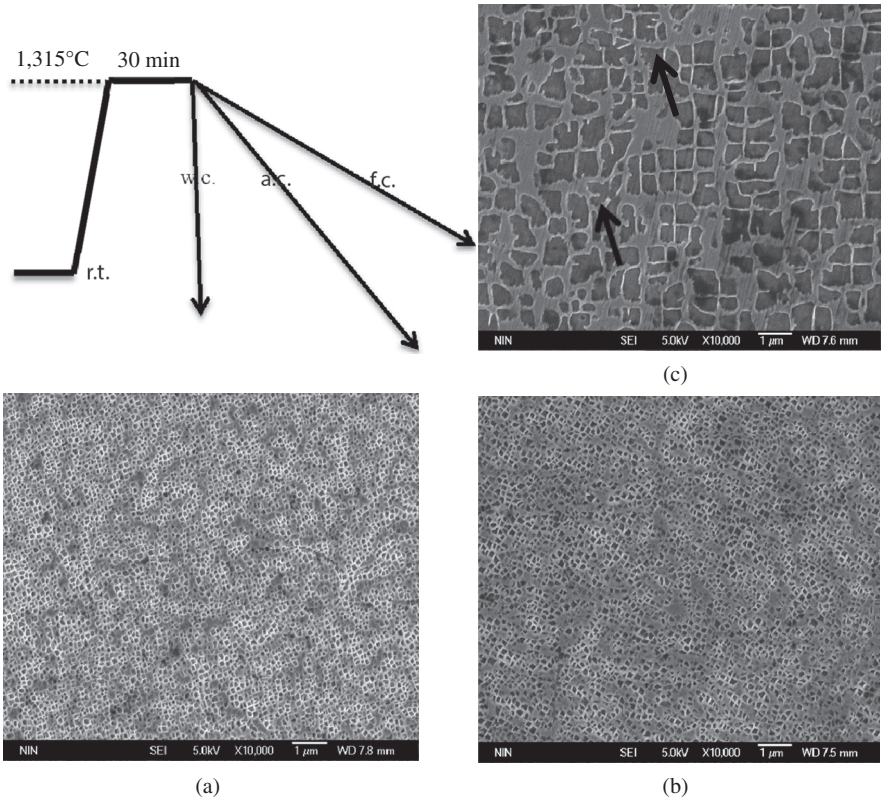

Figure 3: The effect of different cooling rates on the formation of the γ' morphology after isothermal treatments at 1,315°C for 30 min: (a) water cooling; (b) air cooling; (c) furnace cooling.

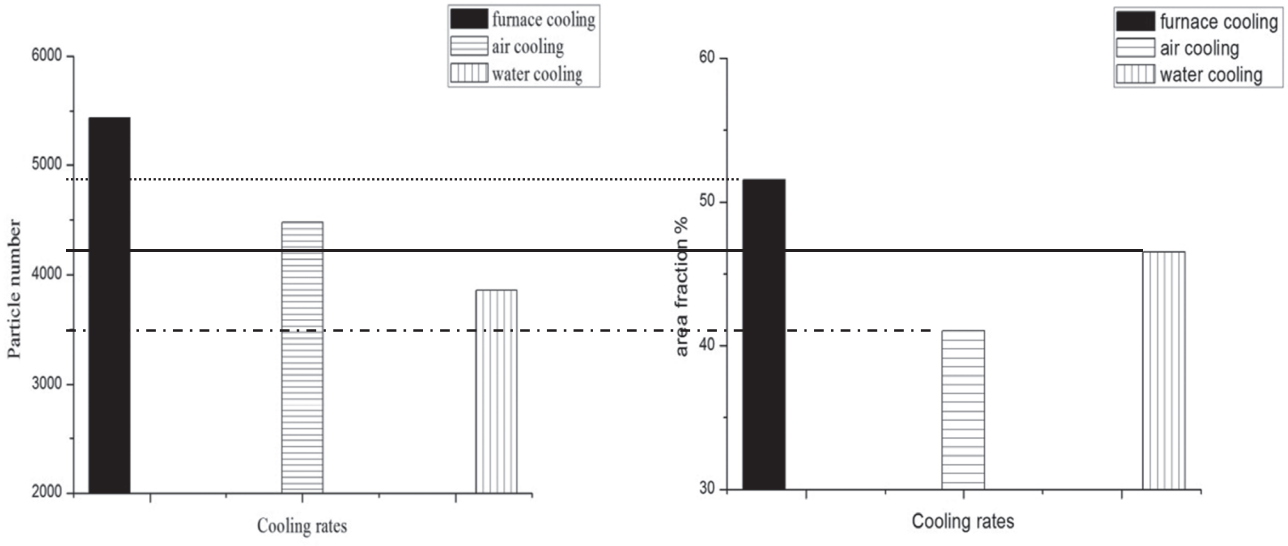

Figure 4: Particle number and volume fraction of γ' precipitates in different cooling rates.

detect that the sample that has been water quenched (Figure 5(c)) tends to have a more regular shape of the gamma prime cuboids. At the same time, Figure 5(d) shows that the gamma prime size gets slightly bigger with the cooling rate increases.

Microstructure evolution during precipitation

Figure 6 shows the microstructure of H4hr DD6 samples quenched during precipitation process for a continuous cooling rate of 0.15°C/s sometimes followed by isothermal

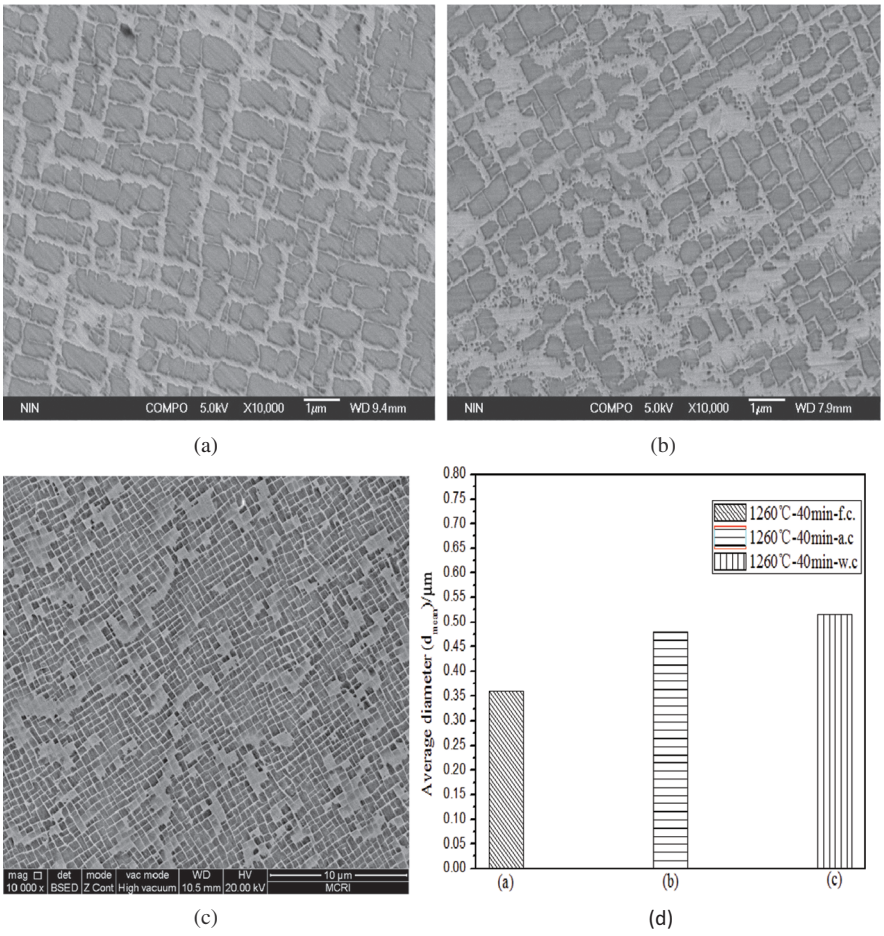

Figure 5: Evolution of precipitate microstructure with isothermal ageing at 1,260°C followed by different quenching rates: (a) continuous heating at 0.15°C/s from room temperature until 1,260°C followed by isothermal treatment for 40 min and then furnace cooling simplified as 1,260°C-40 min-f.c.; (b) 1,260°C-40 min-a.c.; (c) 1,260°C-40 min-w.c. and (d) shows the gamma prime average size for above three quenching conditions.

heat treatments. Isothermal treatment just below the γ' solves made the precipitation proceed randomly throughout the grain in a homogeneous manner, as demonstrated by micrographs 6(a) and (b) from samples quenched at 1,280 and 1,260°C after subsequent isothermal heat treatment, respectively. Among the small spherical precipitates resulting from the quench, the first "resolvable" precipitates had a so-called dewdrop cubic morphology (arrows A in micrograph (a)). In addition to these small cubic morphologies, the precipitates presented three kinds of morphology as a function of their size in the early stage of precipitation. The largest precipitates (arrows D) consisted of a structure of four adjacent trapeziform particles. The "goblet" morphology (arrow B) actually consisted of two small cubic one. The other precipitates (arrows C) consisted of a structure made of particles with fillet angles but attached to each other just like cross. At 1,260°C (micrograph Figure 6(c)), the precipitates have grown in size and protrusions could be observed at the tip of some squared shapes (arrows E). It is rather clear from the succession of micrographs 6(a)–(c) that the different precipitate shapes arrowed A→B→C→D→E→A + D depicts various stages of a splitting process going from a single precipitate (A) to a structure made of adjacent particles (D). As we can see, the particle (E) represents a transition condition that ultimately divides into two parts: a single precipitation (A) and four adjacent particles (D). Visual image is drawn in Figure 7. For further cooling, the clustering phenomenon was observed (arrow F) in Figure 6(d), compared with the structure of four adjacent "square" particles (arrow D), this morphology (arrow F) contains more particles in number as well as more complicated characteristic in formation. The formation of clustering is more or less related to the specific quenching temperature (1,240°C); furthermore, it is the quenching temperature that leads the γ' particles to a rapid growth in narrow local area and those small particles are not ready for uniform distribution in the following water cooling. In comparison to Figure 6(f), the precipitates shown in Figure 6(e) had a slightly bigger size and their morphology seemed to be more uniform. This

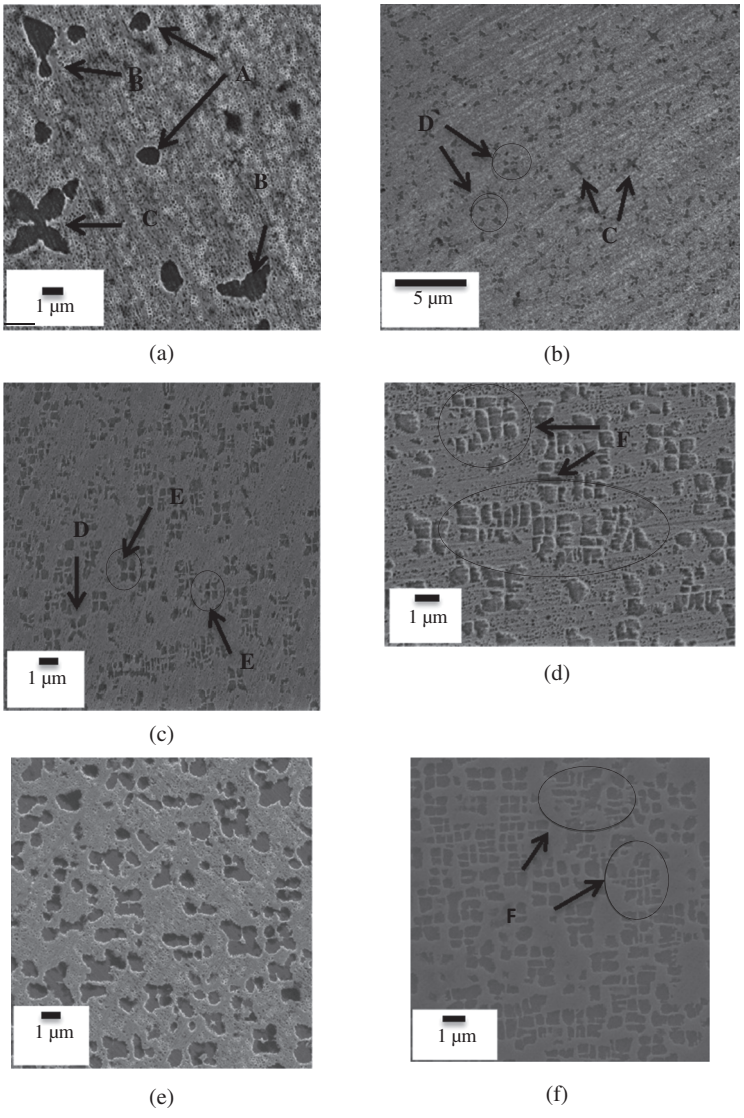

Figure 6: SEM micrographs showing the microstructure of samples quenched during the precipitation process after a continuous cooling at 0.15°C/s or continuous cooling followed by isothermal treatments for the H4hr DD6 superalloy. (a) Isothermal treatments at 1,315°C for 30 min, and continuous cooling at 0.15°C/s followed by isothermal treatments at 1,280°C for 40 min and then water cooling on DD6 specimens (simplified as 1,280°C-40 min); (b) 1,260°C-40 min; (c) Isothermal treatments at 1,315°C for 30 min, and continuous cooling at 0.15°C/s until 1,260°C followed by water cooling on DD6 specimens (simplified as 1,260°C); (d) 1,240°C; (e) 1,220°C-40 min; (f) 1,220°C.

shows that isothermal heat treatment makes for the growth as well as the orderly arrangement of precipitates, which is consistent with the conclusion mentioned above, actually. In addition, clustering has not been found in Figure 6(e), it is the elastic field existed in every between γ' precipitate forces those particles to be uniform from clustering condition.

Dissolution

Figure 8 shows micrographs of specimens quenched during heating (0.15°C/s) or after an isothermal ageing at 1,240°C for 80 min. While in some areas precipitates have dissolved or were undergoing a dissolution process (arrows A), in other areas stable precipitates aligned along the <001> directions were still existent (arrows B). More information about the comments specific to the fine scale structure of the γ' precipitates under dissolution can be found in Ref. [7]. After 80 min at 1,240°C the precipitates had lost their cubic shape for a more rounded one (see Figure 8(d)).

Discussion

Volume fraction

The quantitative image analysis results in Figure 1(a) indicates that the volume fraction of γ' phase under dissolution was further away from equilibrium than under precipitation, which is in agreement with Grosdidier [10]. Although the volume fraction of γ' phase under

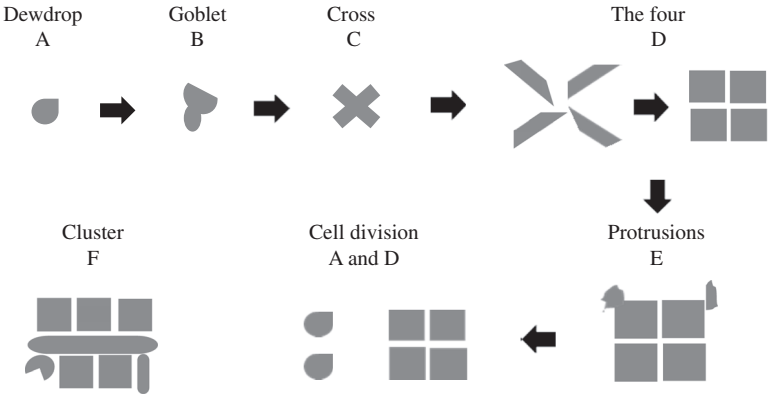

Figure 7: Various stages of a splitting process going from a single precipitate (A) to a structure made of adjacent particles (D). Protrusion (E) is a transition condition. Cluster (F) is observed in Figure 6(d) and 6(f).

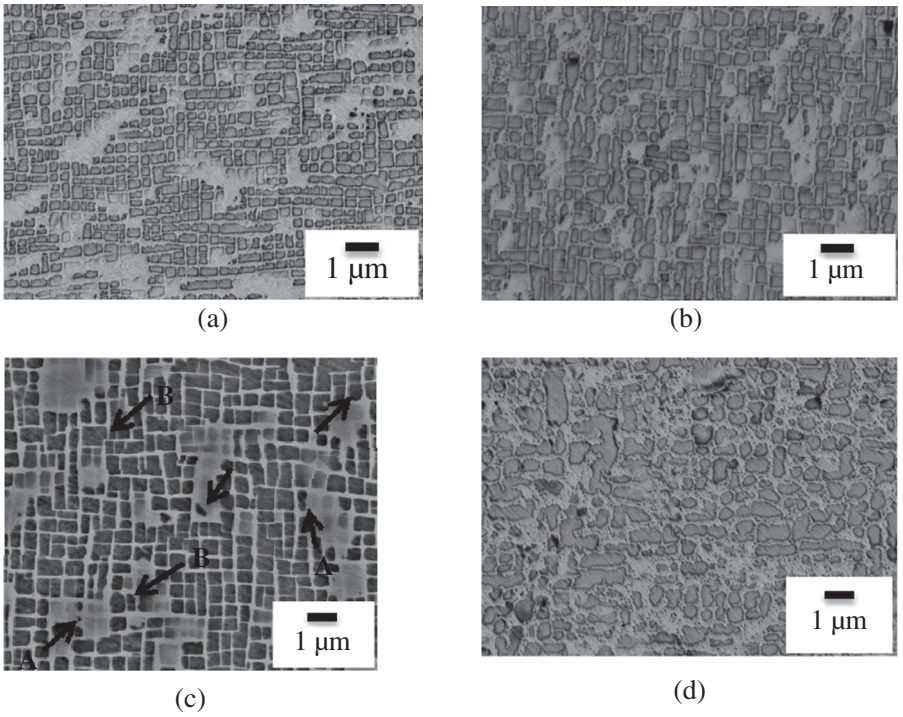

Figure 8: (a)–(d) SEM micrographs showing the microstructure of samples quenched during the dissolution process after a continuous heating at 0.15°C/s (a), (b) and (c) or continuous heating followed by isothermal treatment at 1,240°C for 80 min. (d)H4hr DD6 superalloy. (a) continuous heating at 0.15°C/s from room temperature until 1,170°C and then water cooling (simplified as 1,170°C); (b) 1,240°C; (c) 1,260°C; (d) continuous heating at 0.15°C/s from room temperature until 1,240°C followed by isothermal treatment for 80 min and then water cooling (simplified as 1,240°C-80 min).

dissolution could be slightly over-estimated because a possible increase in volume fraction during the quenching process cannot be eliminated, it is doubted whether this deviation from the equilibrium could be attributed to the fact that the coherent γ' precipitates withstand dissolution.

Gamma prime size distribution: ageing and cooling rates

The γ' precipitates are major strengthening phases in the superalloys. They coherently precipitate from the γ matrix during the cooling process. Figure 2(a) shows a

rather interesting distribution of γ' with a spherical "labyrinth morphologies", regrettably, similar morphology has not been found in other documents. There is a doubt that this reveals the splitting mechanisms in unknown manner.

Precipitation

For the cooling rate of 0.15°C/s set in this work, a main part of the precipitates grown freely until the octocubic stage (Figure 4). In fact, their precise shape during cooling due to an equilibrium between effects related to elastic strain and others resulting from kinetics of diffusion. The matrix is supersaturated in the initial stage of the precipitation process and, for kinetics effects, the precipitates are "dewdrop" and "goblet" in shape, although this is not an equilibrium shape from a merely elastic point of view [11]. Precipitates emerging branches attached to one another (the "cross") are metastable structures of precipitates growing rapidly in a supersaturated matrix while undergoing splitting. Next in the process, when growth is delayed by the effect of the diffusion field, the precipitate interfaces tend to the equilibrium flat ones. At this stage, further increase in the γ' volume fraction can also be achieved by the growth of new precipitates (i.e. dewdrop) in the depleted γ corridors [10].

Dissolution

The observations show that the dissolution process of the γ' phase is also intensely affected by the presence of the elastic field associated with the misfit. The preferential selection of the precipitates to dissolve is determined by differences in local stability associated with the elastic interactions. The dissolution of the γ' precipitates is related to the consecutive disappearance of precipitate groups tending to be unstable to others [7]. Because of this, small precipitates within the alignment have to grow at the cost of larger ones which are not in an actively favorable position. In a similar way, coherency strain was shown to be accountable for preferential coarsening under ageing in other alloys. This was demonstrated by the point that small precipitates did not dissolve all for the growth of larger precipitates [6]. Without large enough elastic strain field, the dissolution process is far more continuous and uniform. This was observed when the dissolution process was carried out under applied stress so that a dislocation network could form at the γ/γ' interface [7].

Conclusions

The effect of post-heat treatment on the microstructures in commercial material DD6 is fully investigated. The following conclusions can be drawn from this work:

- The major part of the transformation occurs in the range from 1,120°C to 1,315°C. Though the moderate cooling and heating rate of 0.15°C/s are selected in this work, noticeable deviation from the equilibrium volume fraction of γ' phase is detected for both the dissolution and precipitation processes above 1,120°C.
- Figure 2(b)–(c) shows the evolution of the structure with ageing time. They indicate that ageing time contributes to both the size and ordered distribution of γ' phase.
- Lower cooling rate make for the growth as well as an ordered arrangement of γ' precipitates when samples quenched at 1,315°C; comparatively, under the condition of continuous heating at 0.15°C/s from room temperature to 1,260°C, it is not difficult to conclude that the quicker the cooling rate is, the bigger size and ordered arrangement of γ' precipitates will get.
- Specific quenching temperature (1,240°C in this paper) contributes to the clustering of γ' precipitates.
- The experimentally defined shape sequences are as follows: Dewdrop→ Goblet→ Cross→ The four→ Protrusions. The consecutive shape changes witnessed during precipitation can be understood by considering the consecutive equilibrium shapes of a precipitate which grows initially in an infinite matrix. In addition, the phenomenon of cluster in local area can be attributed to the elastic field between γ' precipitates and its neighbors.
- Providing that the γ' precipitates stay coherent, the choice of the precipitates to dissolve first is determined by differences in local stability related to the elastic interactions. It is also illustrated that the coherency of the precipitates improves their potential to resist dissolution.

Acknowledgments: The authors wish to thank Xi'an Modern Chemistry Research Institute and Northwest Research Institute of nonferrous metals for SEM analysis.

Funding: We are grateful for the financial support provided by the NSFC (51210008) and Innovation Seed Fund for Graduate Student of Northwestern Polytechnical University (Z2014046).

References

[1] F. Cosentino et al., J. Mater. Process Technol., 213 (2013) 2350–2360.
[2] R.A. Ricks, A.J. Porter and R.C. Ecob, Acta Metall., 31 (1983) 43–53.
[3] M.V. Nathal and R.A. Mackay, Mater. Sci. Eng., 85 (1987) 127–138.
[4] J.G. Conley, M.E. Fine and J.R. Weertman, Acta Metall., 37 (1989) 1251–1263.
[5] A. Maheshwari and A.J. Ardell, Acta Metall. Mater., 40 (1992) 2661–2667.
[6] A.D. Sequeira, H.A. Calderon and G. Kostorz, Scr. Metall. Mater., 30 (1994) 7–12.
[7] T. Grosdidier, A. Hazotte and A. Simon, Scr. Metall. Mater., 30 (1994) 1257–1262.
[8] S. Kraft, I. Altenberger and H. Mughrabi, Scr. Metall. Mater., 32 (1995) 411–416.
[9] Y.Y. Qiu, Acta Mater., 44 (1996) 4969–4980.
[10] T. Grosdidier, A. Hazotte and A. Simon, Mater. Sci. Eng. A, 256 (1998) 183–196.
[11] A. Hazotte, T. Grosdidier and S. Denis, Scr. Mater., 34 (1996) 601–608.
[12] M. Cornet and G. Martin, Scr. Metall., 21 (1987) 1091–1095.
[13] A.G. Khachaturyan, S.V. Semenovskaya and J.W. Morris Jr, Acta Metall., 36 (1988) 1563–1572.
[14] J.F. Ganghoffer et al., Scr. Metall. Mater., 25 (1991) 2491–2496.
[15] L. Müller, U. Glatzel and M. Feller-Kniepmeier, Acta Metall. Mater., 40 (1992) 1321–1327.
[16] P.W. Voorhees, G.B. McFadden and W.C. Johnson, Acta Metall Mater., 40 (1992) 2979–2992.
[17] Z. Shi et al., Trans. Nonferrous Met. Soc. China, 21 (2011) 998–1003.
[18] W. Ming-Gang, T. Su-Gui, Y. Xing-Fu and Q. Ben-Jiang, J. Mater. Metall., 8 (2009) 281–286.
[19] Z. Zhong-Kui, W. Bai-Zhi, L. Da-Shun, W. Zhi-Xun and Y. Zhu-Feng, J. Mater. Sci. Eng., 30 (2012) 375–379.
[20] H. Fu-Xiang, W. Jia-Zheng, W. Bing-Lin et al., China Aeronautical Materials Handbook, China Standards Press, Beijing (2002), pp. 812–818.
[21] P. Li et al., Mater. Sci. Eng. A, 603 (2014) 84–92.